Electronic structure, BIS, core-level XPS and XAS in $CePd_7$: experimental and theoretical studies

1993 J. Phys.: Condens. Matter 5 5841

(http://iopscience.iop.org/0953-8984/5/32/013)

J. Phys.: Condens. Matter 5 (1993) 5841–5850. Printed in the UK

Electronic structure, BIS, core-level XPS and XAS in $CePd_7$: experimental and theoretical studies

E Beaurepaire†, J P Kappler†, S Lewonczuk†, J Ringeissen†, M A Khan†, J C Parlebas†, Y Iwamoto‡ and A Kotani‡

† Institut de Physique et Chimie des Materiaux de Strasbourg (UMR 46 CNRS), Université Louis Pasteur, 4 rue Blaise Pascal, 67070 Strasbourg, France

‡ Institute for Solid State Physics, University of Tokyo, 7-22-1 Roppongi, Minato-ku, Tokyo 106, Japan

Received 29 March 1993, in final form 17 May 1993

Abstract. The electronic structure of $CePd_7$ is studied using various spectroscopic techniques (BIS, 3d/XPS and 2p/XAS). The strong delocalization of the Ce 4f electrons, previously suggested by low-temperature specific heat and magnetic susceptibility measurements, is consistent with the spectra we present here. A standard LMTO band structure calculation is performed in the case of $CePd_7$ and its reference compound YPd_7. The bands thus determined, especially the last valence and first conduction bands, mostly arising from Pd 4d and Ce 4f states, are actually hybridized; they provide a good description of the density of states at the Fermi level and a qualitative agreement with BIS spectra. Furthermore the occurrence of satellites in core-level spectra indicates a fairly strongly correlated nature of the 4f states in $CePd_7$. In the next step, the information contained in the LMTO density of states is used to build an impurity Anderson Hamiltonian which incorporates the various Coulomb interactions necessary to analyse the above-mentioned spectroscopic processes within a single set of parameter values for $CePd_7$. Limits and relevance of both theoretical models are discussed.

1. Introduction

Extremely low values of the static magnetic susceptibility χ_0, the specific heat coefficient γ and the χ_0/γ ratio have been reported recently for $CePd_7$ [1,2]; these values are smaller than those previously obtained for α-Ce and other Ce compounds. The case of $CePd_7$ is in strong contrast to the heavy-fermion case [3,4] and is even at the border of the intermediate-valence regime [5]. In fact, the electronic density of states (DOS) that agrees with the χ_0/γ ratio for $CePd_7$ compounds, i.e. $\chi_0/\gamma = 0.012$ emu K^2 J^{-1} [2], corresponds to a system with fairly free conduction electrons, like in light alkaline metals, rather than a typical system of intermediate-valence Ce compounds. This situation suggests a very important delocalization of the Ce 4f electrons. A similar situation has been found for bulk $CeIr_2$ [6] and $CeRh_3$ [7] where the 4f levels should be considered to be more strongly hybridized than previously anticipated, in agreement with an appreciable band-like character of the Ce 4f states.

In this paper our purpose is to present a combined study of the electronic structure of $CePd_7$, as well as its reference compound YPd_7, in order to better recognize the delocalization of the f band and its hybridized character. First we summarize joint experimental results on isochromat and core level spectroscopies: BIS, 3d-XPS and 2p-XAS (section 2). Next we calculate the DOS of $CePd_7$ (as well as that of YPd_7) by using a standard 'linear muffin tin orbitals' (LMTO) band structure computation (section 3). In

0953-8984/93/325841+10$07.50

section 4, taking into account semi-quantitatively the preceding LMTO-DOS, we propose to model the electronic structure of $CePd_7$ and analyse the various experimental spectra of section 2 in a consistent way by using an impurity Anderson model [8–11]. Finally, section 5 is devoted to a general discussion with concluding remarks.

2. Experimental study of BIS, 3d-XPS and 2p-XAS

2.1. Experiments

The sample preparation and characterization of $CePd_7$ and YPd_7 phases as the experimental L_{III} edge (2p-XAS) have been presented elsewhere [1]. BIS and 3d-XPS spectra were recorded in separate UHV chambers (base pressure 1×10^{-10} Torr). The samples have been cleaned *in situ* by Ar sputtering and then annealed at 400 °C in order to restore the surface, avoiding phase separation. The sample cleanliness was checked by monitoring XPS or Auger lines. 3d core level XPS spectra are recorded from the Al-Kα line using the V G Clam electron analyser (the total apparatus resolution is 0.8 eV full width at half maximum). BIS data are obtained at a fixed photon energy of 1487 eV (the principle of the apparatus is the same as in [12]). Typical incident electron current is 0.4 mA and the total instrumental resolution is estimated to be 0.7 eV from the width of the Cu Fermi level. The spectra are recorded while cooling the sample from room temperature down to 77 K in order to delay its degradation that occurs typically within one hour.

2.2. Results

The BIS spectra of $CePd_7$ and of the isostructural f-electronless compound YPd_7 are represented with an energy scale extending 20 eV above the Fermi energy (figure 1). Similar structures in $CePd_7$ and YPd_7 are observed centred around 4 and 14 eV above the Fermi level. However, the structures close to the Fermi level are very different, since a large peak is observed for $CePd_7$ at 1 eV, whereas only a small peak emerges from the Fermi edge in the case of YPd_7. These features will be discussed in more detail in section 5.

The experimental Ce 3d-XPS spectrum is reported on figure 2. The complicated line shape is typical of Ce mixed valence systems. In order to have a qualitative understanding of such spectra, one has to consider that the ground state is a mixture of nearly degenerate $4f^0$ and $4f^1$ configurations, whereas, because of screening effects, the $4f^2$ and $4f^1$ are stabilized in the presence of a 3d core-hole. Moreover, this manifold of final state split lines is replicated by the spin–orbit splitting of Ce 3d core levels (about 18 eV) in the present case. The corresponding assignment of the peaks is labelled on figure 2. Notice the overlap between $3d_{5/2}\,4f^0$ and $3d_{3/2}\,4f^2$ final states. The separation between the $4f^0$ and the $4f^1$ peak gives an estimation of the Coulomb interaction (U_{cf}) between a 4f electron and the core-hole; the separation $4f^2$–$4f^1$ amounts roughly to the difference U_{cf}–U_{ff} (U_{ff} denotes the Coulomb interaction between f electrons). Quantitative calculations within the Anderson impurity model [8, 10] (see section 4) show that the relative intensity of the $4f^0$ peak is related to the importance of the hybridization between 4f and conduction states and that it scales with the fractional occupancy of 4f orbitals in the ground state.

Finally the measured L_{III} XAS edge of Ce in $CePd_7$ is given in figure 3. In common with other mixed valence Ce systems, the XAS spectrum exhibits a double-peaked structure [9, 10]. The interpretation of these data is similar to the previous one, the $4f^0$ peak appearing around 5732 eV and the $4f^1$ around 5725 eV. However, one should notice the exceptional intensity of the $4f^0$ structure since a phenomenological analysis of the line shape leads to a Ce valence $v \simeq 3.5$ [1].

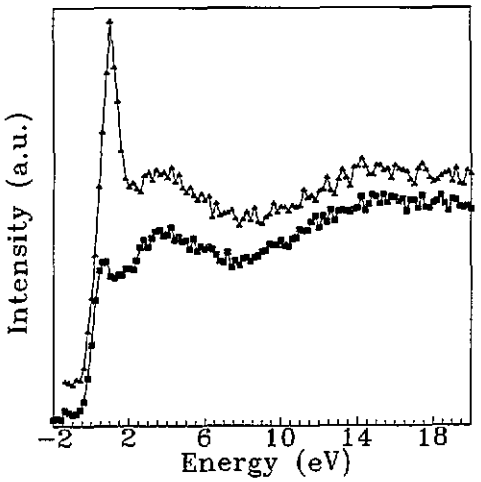

Figure 1. Experimental BIS of $CePd_7$ (upper curve) and YPd_7 (lower curve).

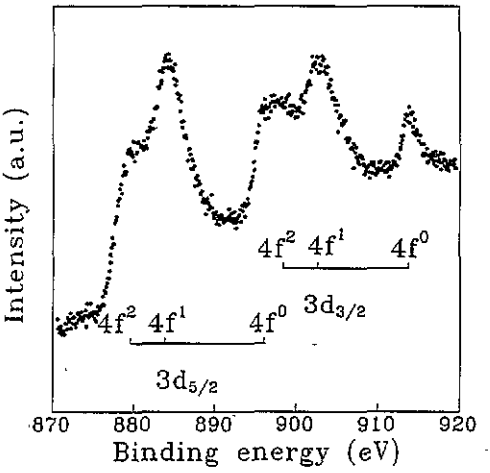

Figure 2. Experimental Ce 3d-XPS of $CePd_7$ recorded with Al-Kα radiation ($h\nu = 1487$ eV).

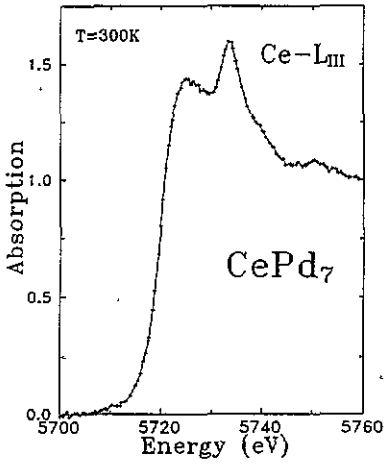

Figure 3. Experimental Ce L_{III} XAS of $CePd_7$.

3. Energy band calculation

The LMTO method [13] in atomic sphere approximation (ASA), with combined corrections included, has been successfully used to calculate the electronic structure of RPd_3 (R = Y, Ce) [14]. Most of the observed physical properties of RPd_3 were well explained in an energy band scheme. A similar theoretical study is extended here to RPd_7. The RPd_7 compound is composed of eight FCC sublattices [15] with 8.096 Å and 7.940 Å as the lattice constants for $CePd_7$ and YPd_7 respectively [1, 16]. Each R atom is surrounded by 12 Pd nearest neighbours (NN). Out of 7 Pd atoms, one Pd (Pd I) has 12 Pd NN atoms whereas each Pd (Pd II) of the remaining six has 2 R and 10 Pd NN atoms. The starting atomic potential is constructed with $4f^2\,5d^0\,6s^2$ for Ce, $4d^1\,5s^2$ for Y and $4d^{10}\,5s^0$ for Pd as the conduction electrons. The core levels are considered frozen. We consider the muffin tin orbitals of angular momentum s, p, d and f for each atom. The exchange correlation of von Barth–Hedin [17] is used as the local density approximation (LDA).

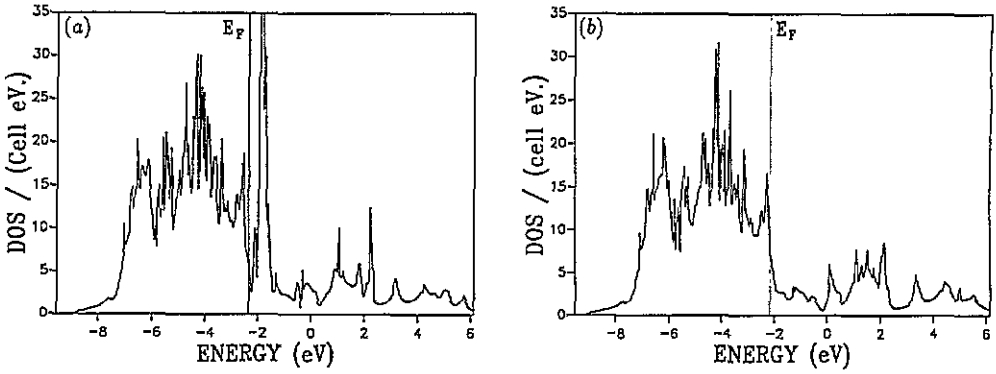

Figure 4. Total DOS of (*a*) $CePd_7$ and (*b*) YPd_7 obtained from LMTO band calculation.

Table 1. Total DOS/eV at the Fermi level $n(E_F)$, contributions from different atomic spheres $n^X(E_F)$ (X = R, Pd I, Pd II), charge variation ΔQ^X in the X atomic sphere and '*a*', the *corresponding lattice constants in atomic units.*

	YPd_7	$CePd_7$
$n(E_F)$	7.287	5.706
$n^R(E_F)$	0.076	1.066
$n^{Pd\ I}(E_F)$	0.970	0.831
$n^{Pd\ II}(E_F)$	1.040	0.634
ΔQ^R	1.050	1.122
$\Delta Q^{Pd\ I}$	−0.040	−0.084
$\Delta Q^{Pd\ II}$	−0.168	−0.173
a (au)	15.009	15.304

In figures 4(*a*) and (*b*) we present the total DOS/eV cell in $CePd_7$ and YPd_7 respectively. Figures 5(*a*) and (*b*) show the local DOSs in the Ce atomic sphere (AS) and the Y AS for these compounds. In table 1 we give different DOSs at the Fermi level and the charge variations in different ASs for $CePd_7$ and YPd_7. In the case of $CePd_7$ there is an intense high density peak (figures 4(*a*) and 5(*a*)) in the unoccupied region just above the Fermi level at a distance of 0.55 eV. This peak is of Ce 4f origin (figure 5(*a*)). This structure is obviously absent in YPd_7 (figure 5(*b*)). Towards the higher-energy side the empty states are mainly of R 5d origin. When the BIS of YPd_7 and $CePd_7$ (figure 1) are compared, the intense peak, just at the threshold, observed in the case of $CePd_7$ is readily understood from the present band scheme.

It is interesting to note that $n(E_F)$ in $CePd_7$ is smaller than the corresponding value in YPd_7. This entails a smaller specific heat coefficient, γ, for $CePd_7$ than for YPd_7, in agreement with the experimental results [1]. Notice that, in the case of RPd_3, it was found that $\gamma(CePd_3) > \gamma(YPd_3)$ [14]. From energy band calculations, it appears that the 4f states are less localized in $CePd_7$ than in $CePd_3$ [14] and thus the mixed-valence effect observed in $CePd_3$ is absent in $CePd_7$. One should notice that the shape of this L_{III} edge is exceptional for Ce compounds as far as the intensity of the $4f^0$ structure is concerned.

4. Impurity Anderson model and theoretical analysis of the spectra

A theoretical analysis of BIS, 3d-XPS and 2p-XAS for $CePd_7$ compounds is here performed within the impurity Anderson model and in the lowest approximation of the $1/N_f$ expansion.

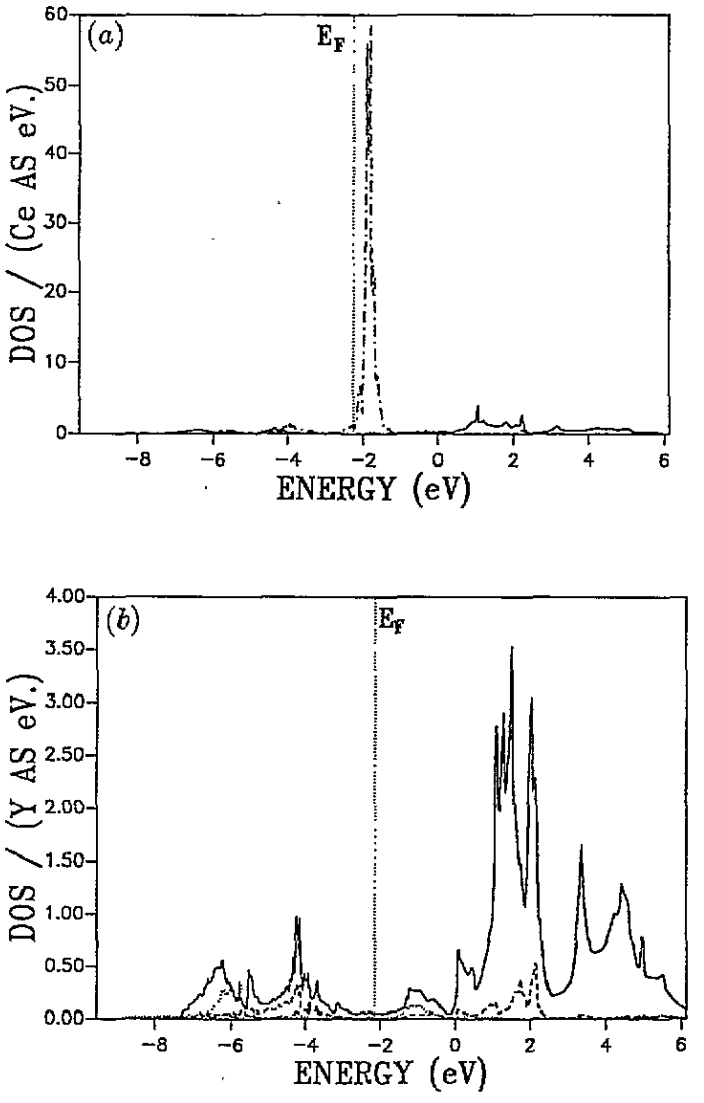

Figure 5. Partial DOS of (*a*) $CePd_7$ in the Ce atomic sphere; and (*b*) YPd_7 in the Y atomic sphere; s, p, d and f symmetries appear respectively as dotted (·····), dashed (----), continuous (——) and dashed-dotted (— · —) curves.

We represent the total DOS of $CePd_7$ (figure 4(*a*)) obtained in section 3 by an electron system consisting of an almost filled valence band (VB; essentially: Pd 4d states), an empty conduction band necessary for the absorption process (CB; for simplicity: Ce 5d states) and a Ce 4f level as well as a Ce core level (3d or 2p levels for XPS or XAS, respectively). The Hamiltonian of the system is then expressed as

$$H = \sum_{k,\nu} \epsilon_{VB}(k) a^+_{VB}(k,\nu) a_{VB}(k,\nu) + \sum_{k} \epsilon_{CB}(k) a^+_{CB}(k) a_{CB}(k)$$

$$+ \epsilon^0_f \sum_{\nu} a^+_f(\nu) a_f(\nu) + \epsilon_c a^+_c a_c + \frac{V}{N^{1/2}} \sum_{k,\nu} (a^+_{VB}(k,\nu) a_f(\nu) + \text{hc})$$

$$+ U_{ff} \sum_{\nu>\nu'} a_f^+(\nu) a_f(\nu) a_f^+(\nu') a_f(\nu') + \frac{U_{fd}}{N} \sum_{k,k',\nu} a_f^+(\nu) a_f(\nu) a_{CB}^+(k) a_{CB}(k')$$

$$- (1 - a_c^+ a_c)\left(U_{fc} \sum_{\nu} a_f^+(\nu) a_f(\nu) + \frac{U_{dc}}{N} \sum_{k,k'} a_{CB}^+(k) a_{CB}(k') \right)$$

where $\epsilon_{VB}(k)$, $\epsilon_{CB}(k)$, ϵ_f^0 and ϵ_c are the energies of the VB, CB, 4f level and core level, respectively; $a_{VB}^+(k;\nu)$, $a_{CB}^+(k)$, $a_f^+(\nu)$ and a_c^+ are the electron creation operators in these states. Here k denotes the index of the energy level ($k = 1, \ldots, N$) in the VB and CB and ν specifies both the spin and orbital degeneracies ($\nu = 1, \ldots, N_f = 14$). V is the hybridization between the Ce 4f level and the VB Pd 4d states. U_{ff} is the Coulomb interaction between 4f electrons whereas $-U_{fc}$ ($-U_{dc}$) is the core-hole potential acting on the Ce 4f electron (Ce 5d electron): c ≡ 3d for XPS, c ≡ 2p for XAS and $a_c^+ a_c = 1$ in the initial and final states of BIS. The spin and orbital degeneracies in ϵ_c and each of $\epsilon_{CB}(k)$ are disregarded, since they are not essential in the present analysis. In the calculation we confine ourselves to the subspace containing $4f^0$, $4f^1L$ and $4f^2L^2$ configurations in the ground state where L labels a hole in the VB. Also the realistic bands of section 3 are replaced by finite numbers of levels, the energies of which are

$$\epsilon_{VB}(k) = \epsilon_{VB}^0 - W_V/2 + (k - \tfrac{1}{2}) W_V/N \qquad \epsilon_{CB}(k) = \epsilon_{CB}^0 - W_d/2 + (k - \tfrac{1}{2}) W_d/N$$

where the half-widths W_v and W_d of the VB and CB are semi-quantitatively taken according to the preceding band structure calculation (see table 2). We denote the ground state of H with the energy E_g and with $a_c^+ a_c = 1$ by $|g\rangle$. For the BIS process, when one electron is added above the Fermi level due to the incident electron, the system state changes to the final state of the BIS: $|f(BIS)\rangle$ with energy $E_f(BIS)$ and the corresponding spectrum is

$$F_{BIS}(E) = \sum_f \sum_\nu |\langle f(BIS)|a_f^+(\nu)|g\rangle|^2 L(E - E_f(BIS) + E_g).$$

For simplicity, we disregard the creation of a Ce 5d electron ($a_{CB}^+(k)$) in BIS. When a 3d core electron is excited (by absorbing an incident photon) to a high energy photoelectron state, the state $|g\rangle$ changes to the final state of the 3d-XPS, $|f(XPS)\rangle$ with $a_c^+ a_c = 0$ and with the energy $E_f(XPS)$; the corresponding spectrum is then

$$F_{XPS}(E_B) = \sum_f |\langle f(XPS)|a_c|g\rangle|^2 L(E_B - E_f(XPS) + E_g).$$

Finally when a 2p core electron is absorbed into the CB Ce 5d states, the system state $|g\rangle$ changes to the final state of the L_{III}-XAS, $|f(XAS)\rangle$, with the energy $E_f(XAS)$ (and with $a_c^+ a_c = 0$); the absorption spectrum is

$$F_{XAS}(\omega) = \frac{1}{N} \sum_f |\langle f(XAS)| \sum_k a_{CB}^+(k) a_c |g\rangle|^2 L(\omega - E_f(XAS) + E_g).$$

In the final states of the absorption process, the Coulomb interaction $-U_{dc}$ between the absorbed Ce 5d electron and the 2p core hole is taken into account as well as U_{fd} between the 5d and 4f electrons.

In all spectroscopic spectra $L(X) = \Gamma/[\pi(X^2 + \Gamma^2)]$. In F_{XPS} and F_{XAS} the broadening Γ is given in table 2. In F_{BIS}, the spectral broadening Γ is replaced by $\Gamma' = \Gamma_0 + \Gamma_1 |E - \epsilon_F|^2$

Table 2. Parameter values of the impurity Anderson model (eV) and calculated n_f.

$CePd_7$ Parameter	Value (eV)
$\epsilon_f^0 - \epsilon_F$	−1.5
U_{fc}	10.9
U_{ff}	6.8
U_{fd}	1.0
U_{dc}	2.0
V	0.53
W_V	6.0
W_d	6.0
Γ	1.8
Γ_0	0.48
Γ_1	0.031
n_f	0.73

where ϵ_F is the Fermi energy which is taken at the top of the VB ($\epsilon_F = \epsilon_{VB}^0 + W_V/2$), and ($\Gamma_0$, Γ_1) are also given in table 2.

The calculated results for BIS, 3d-XPS and L_{III} XAS are shown in figures 6, 7 and 8, respectively. The origin of the abscissa of figures 7 and 8 is taken arbitrarily. The parameter values, used in the calculations, are listed in table 2. From these parameter values, the average 4f electron number in the ground state is estimated to be $n_f = 0.73$. For 3d-XPS and L_{III} XAS, the background contributions (the broken lines in figures 7 and 8) are taken into account by the expressions

$$B_{XPS}(E_B) = C\int_{-\infty}^{E_B} F_{XPS}(E'_B)\,dE'_B$$

$$B_{XAS}(\omega) = C'\int_{\Delta}^{\infty} \exp[-\alpha(\epsilon - \Delta)]F_{XPS}(\omega - \epsilon)\,d\epsilon$$

where C, C', α and Δ are taken appropriately as adjustable parameters.

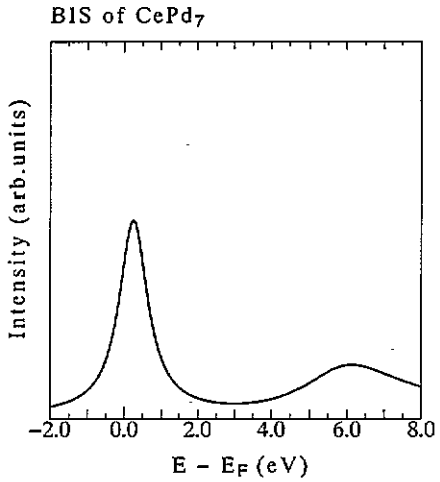

Figure 6. Calculated BIS (f contribution) of $CePd_7$ within the impurity Anderson model.

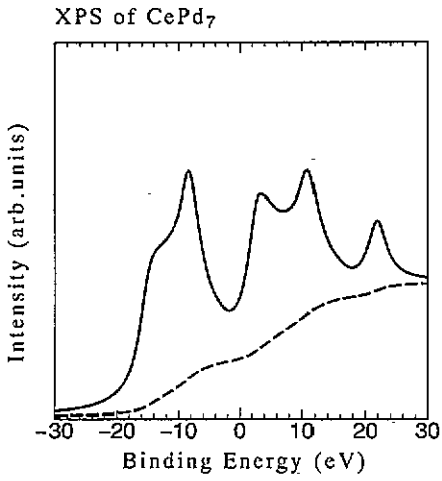

Figure 7. Calculated Ce 3d XPS of $CePd_7$ within the Anderson model and including a background contribution.

The reason why the experimental 4 eV BIS peak does not show at all in the impurity Anderson model calculation is that this peak originates mainly from the Ce 5d band contribution which has been disregarded in the (BIS) Anderson model but is clearly seen in the band calculation. In our calculations, the parameter values (table 2) are estimated to best reproduce the experimental result of 3d-XPS. Then, the agreement between theory and experiment is less satisfactory for BIS and L_{III} XAS; the higher energy component of BIS is too strong, and the higher energy peak of L_{III} XAS is too weak, compared with the experimental data. Some discussion on this point will be given in section 5.

5. Discussion and concluding remarks

We want now to address the limits and relevance of the above-proposed theoretical models (Anderson impurity and band structure calculation) in order to describe the properties of $CePd_7$ and related compounds. As mentioned in chapter 3, band structure calculations provide estimates of the density of states at the Fermi level $n(E_F)$ in fairly good agreement with experimental values of the magnetic susceptibilities and Sommerfeld coefficients for $CePd_7$ and YPd_7. However, the electrons at the Fermi level are mainly of s–p–d origin, so that, from the analysis of the band structure, $n(E_F)$ is mainly representative of the filling of the Pd 4d bands. Fruitful information is obtained from the comparison of calculated and experimental density of empty states. The upper part of figure 9 represents, from top to bottom, the total DOS in $CePd_7$, the s–p–d DOS in $CePd_7$ and the total DOS in YPd_7 (the theoretical DOSs of $CePd_7$ and YPd_7 have been truncated at the Fermi level and convoluted with a Gaussian function (FW = 0.7 eV) in order to enable the comparison with experiments). The lower part represents (also from top to bottom) the experimental BIS of $CePd_7$, the experimental BIS of YPd_7 and the difference in these two spectra in order to extract the 4f contribution in the density of empty states. The good overall agreement between theory and experiment allows us to assign:

(i) the bump close to the Fermi level in YPd_7 to the vacant states in Pd 4d bands;
(ii) the intense peak in $CePd_7$ to the 4f states;
(iii) the broad feature at 4 eV to the nearly empty 5d bands of the Ce or Y element.

A closer inspection of the data reveals a quantitative discrepancy since the Ce 4f band is predicted at 0.55 eV whereas its experimental position is (1 ± 0.1) eV. Note that the experimental position agrees with the $4f^0 \rightarrow 4f^1$ transition observed in similar Ce compounds ($CeCo_2$ [18], $CeRu_2$ [19] or $CeRh_3$ [20]).

Moreover, firstly, the calculated 4f bandwidth amounts to a fraction of an eV, a value roughly an order of magnitude smaller than reasonable estimates obtained from f–f correlation energy in Ce systems, and secondly, satellites are observed in core-level spectra which cannot be explained in a one-electron scheme. Therefore, band structure calculations are not expected to explain all the details in the electronic structure of $CePd_7$.

On the other hand, the impurity Anderson model should be a valid starting point to describe some properties of $CePd_7$ since the direct f–f overlaps are extremely weak due to the peculiar crystallographic structure. However the impurity model is better for core-level spectra (3d-XPS, L_{III} XAS because of core-hole localization) than for BIS. Model calculations presented in the previous section provide an overall description of the spectroscopic experiments with a single set of parameters. A quantitative agreement is obtained for the 3d-XPS spectrum whereas the BIS spectra seem to be better described by the band calculation than by the impurity model. According to figure 6, the position of the

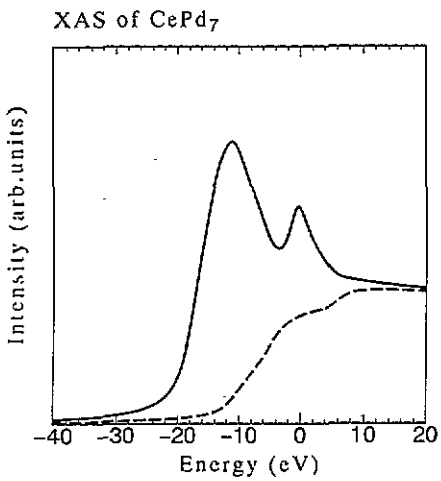

Figure 8. Calculated Ce L_{III} XAS of $CePd_7$ within the impurity Anderson model and including a background contribution.

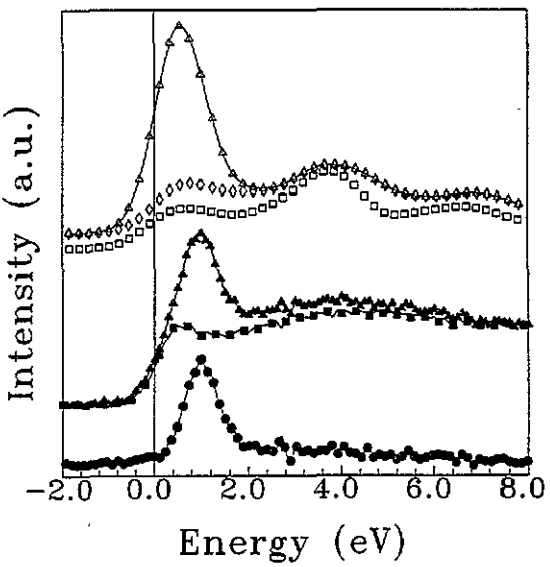

Figure 9. Comparison of experimental BIS and theoretical LMTO densities of empty electronic states for $CePd_7$ and YPd_7, these last densities having been truncated at the Fermi level and folded with a Gaussian function (see text): from top to bottom, the three upper curves represent the total DOS in $CePd_7$, the s–p–d DOS in $CePd_7$ and the total DOS in YPd_7 whereas the three lower curves represent the experimental BIS of $CePd_7$ (figure 1) the experimental BIS of YPd_7 (figure 1) and the difference between these two last spectra.

$4f^0 \rightarrow 4f^1$ peak (0.25 eV) is too close to the Fermi level, and the $4f^1 \rightarrow 4f^2$ peak (near 6 eV) is unresolved in the experimental data mainly because its relative intensity is weak and because it overlaps strongly with band states. This may indicate that the 4f state of $CePd_7$ is delocalized, and that the impurity Anderson model, with the present parameter values, overestimates the correlation effect of the 4f electrons. Another remaining problem is the relative intensity of the high energy $4f^0$ peak of the L_{III} edge (see figures 3 and 8) which is too weak in the calculated spectrum. Two directions could be followed in order to solve this last discrepancy:

(i) a surface contribution from γCe up to about 40% cannot be ruled out in XPS data. If we take into account the surface contribution to 3d-XPS, the estimated $4f^0$ weight in the ground state of the bulk system will increase, and then the $4f^0$ peak intensity of L_{III} XAS will also increase;

(ii) the Anderson Hamiltonian parameters should be renormalized to take into account final state configuration and/or core hole effects [21]. This last point can be in principle relaxed from an *ab initio* calculation of the Anderson model parameters [21] but is beyond the scope of the present study.

To conclude, we have presented an experimental and theoretical study of the electronic structure of RPd_7 compounds (R = Y, Ce). This problem is particularly interesting because hybridization effects are expected to be large [1, 2] and because the chemical content of the rare earth is low (12.5%) so that the one impurity Anderson model is expected to be a valid

approximation. We observed that band structure calculation provides a good description of the density of states at the Fermi level and a qualitative agreement with BIS spectra; this indicates the delocalization or hybridization of Ce4f level. However, the occurrence of satellites in core level spectra and the estimated ratio $U_{ff}/W_f \simeq 10$ lead us to the conclusion that 4f states are fairly correlated in $CePd_7$ although a *quantitative* description using the Anderson model is questionable especially for BIS. Also surface effects should probably be included to interpret L_{III} XAS and renormalization of the parameters should be taken into account for each spectroscopy. A more accurate theoretical study would require a more difficult *ab initio* investigation. This conclusion agrees with a recent reinterpretation of the BIS data of the related compound $CeRh_3$ [7] that has been recently proposed [20].

Acknowledgments

The authors would like to thank Mr G Schmerber for the sample preparation, Dr D Malterre for fruitful discussions and the referees for their pertinent remarks.

References

[1] Kappler J P, Besnus M J, Lehmann P, Meyer A and Sereni J G 1985 *J. Less-Common Met.* **3** 261
Sereni J G, Trovarelli O, Schaf J, Schmerber G and Kappler J P 1991 *Modern Phys. Lett.* B **5** 1249
[2] Sereni J G, Trovarelli O, Herr A, Schillé J Ph, Beaurepaire E and Kappler J P 1993 *J. Phys.: Condens. Matter* **5** 2927
[3] Stewart G R 1984 *Rev. Mod. Phys.* **56** 755
Steglich F 1985 *Theory of Heavy Fermions and Valence Fluctuations* ed T Kasuya and T Saso (Berlin: Springer) p 23
[4] Fulde P, Keller G and Zwicknagl G 1988 *Solid State Phys.* **41** 1
Parlebas J C 1990 *Phys. Status Solidi* b **160** 11
[5] Wachter P and Boppart H (eds) 1982 *Valence Instabilities* (Amsterdam: North-Holland)
[6] Laubschat C, Weschke E, Domke M, Simmons C T and Kaindl G 1992 *Surface Sci.* **269/270** 605
[7] Weschke C, Laubschat C, Ecker R, Höhr A, Domke M and Kaindl G 1992 *Phys. Rev. Lett.* **69** 1792
[8] Allen J M, Oh S J, Gunnarsson O, Schönhammer K, Maple M B, Torikachvili M S and Lindau I 1986 *Adv. Phys.* **35** 275
[9] Kotani A, Okada M, Jo T, Bianconi A, Marcelli A and Parlebas J C 1987 *J. Phys. Soc. Japan* **56** 798
Hammoud Y, Parlebas J C and Gautier F 1987 *J. Phys. F: Met. Phys.* **17** 503
[10] Kotani A, Jo T and Parlebas J C 1988 *Adv. Phys.* **37** 37
[11] Miyahara T, Yamazaki T, Kotani A, Arai H, Mitsuishi T, Sugawara H, Fujimori A, Koide T, Sato S and Maezawa H 1990 *J. Phys. Soc. Japan* **59** 3660
[12] Lang J K and Baer Y 1979 *Rev. Sci. Instrum.* **50** 221
[13] Andersen O K 1975 *Phys. Rev.* B **12** 3060
Skriver H L 1984 *The LMTO Method* (Berlin: Springer)
[14] Koenig C 1983 *Z. Phys.* B **50** 33
Besnus M J, Kappler J P, Meyer A 1983 *J. Phys. F: Met. Phys.* **13** 597
Khan M A and Koenig C 1987 *J. Phys. (Paris)* C9 1067
Alouani M, Koenig C and Khan M A 1988 *Solid State Commun.* **65** 327
Koenig C and Khan M A 1988 *Phys. Rev.* B **38** 5887
[15] Smith D A, Jones I P and Harris I R 1982 *J. Mater. Sci. Lett.* **1** 463
[16] Bretschneider T and Schaller H J 1990 *Z. Metallkde* **81** 84
Sakamoto Y, Yoschida M and Flanagan T B 1986 *J. Mater. Res.* **1** 781
[17] Von Barth U and Hedin L 1972 *J. Phys. C: Solid State Phys.* **5** 1629
[18] Hillebrecht F U, Fuggle J C, Sawatzky G A, Campagna M, Gunnarson O and Schonhammer K 1984 *Phys. Rev. B* **30** 1777
[19] Wuilloud E, Bear Y and Maple M B 1992 *Phys. Lett.* **97A** 65
[20] Malterre D, Grioni M and Baer Y comment to [7], to appear in *Phys. Rev. Lett.*
[21] Gunnarsson O and Jepsen O 1988 *Phys. Rev.* B **38** 3568